Mon. Not. R. Astron. Soc. **266,** 227–237 (1994)

Non-linear evolution of density perturbations using the approximate constancy of the gravitational potential

J. S. Bagla★ and T. Padmanabhan★

Inter-University Centre for Astronomy and Astrophysics, Post Bag 4, Ganeshkhind, Pune-411 007, India

Accepted 1993 July 28. Received 1993 July 20; in original form 1993 April 27

ABSTRACT

During the evolution of density inhomogeneities in an $\Omega = 1$, matter-dominated universe, the typical density contrast changes from $\delta \simeq 10^{-4}$ to $\delta \simeq 10^{2}$. During this time, however, the typical value of the gravitational potential generated by the perturbations changes only by a factor of order unity. This significant fact can be exploited to provide a new, powerful approximation scheme for studying the formation of non-linear structures in the Universe. The method evolves the initial perturbation using a Newtonian gravitational potential frozen in time. We carry out this procedure for different initial spectra and compare the results with the Zeldovich approximation and the frozen flow approximation (recently proposed by Matarrese et al.). Our results are in better agreement with the *N*-body simulations than is the Zeldovich approximation. Our approximation also provides a dynamical explanation for the fact that pancakes remain thin during the evolution of density inhomogeneities. While there is some superficial similarity between our results and those of the frozen flow model, they differ considerably in the quality of the velocity information produced. Actual shell crossing does occur in our approximation; there is also motion of particles along the pancakes, leading to further clumping. Some of these features are quite different from those of the frozen flow model. We also discuss the evolution of the density contrast in various approximations.

Key words: galaxies: formation – large-scale structure of Universe.

1 INTRODUCTION

It is generally believed that structures such as galaxies are formed through the growth of density perturbations via gravitational instability. To understand the formation of these structures, it is necessary to evolve the initial perturbations to highly non-linear regimes, which turns out to be a technically formidable task. Usually one applies linear perturbation theory to evolve the inhomogeneities when they are small, but relies on extensive *N*-body simulations to model the non-linear regime. As a result, we have only limited knowledge of the physics of the non-linear regime.

It would therefore be worthwhile to develop semianalytic approximations, which could help us to understand the non-linear evolution of the perturbations. In this paper, we propose one such approximation scheme. We describe its main features and compare its results with some other approximation schemes. After completing this work we came to know of a preprint by Brainerd, Scherrer & Villumsen (1993) in which the same approximation is suggested. We have included a comparison with their work wherever appropriate.

★E-mail addresses for authors: jasjeet@iucaa.ernet.in (JSB); paddy@iucaa.ernet.in (TP).

2 FROZEN POTENTIAL APPROXIMATION (FPA)

To introduce the approximation scheme proposed in this paper, it is best to begin by recalling some well-known theoretical facts. Consider the evolution of a density perturbation δ in the matter-dominated era of an $\Omega = 1$ Friedmann model, described by an expansion factor $a(t)$. It is well known that $\delta \propto a$ for the growing mode, implying that the perturbed Newtonian gravitational potential ϕ (generated by this perturbation) remains constant in time. As evolution proceeds, δ will approach unity, invalidating the application of linear theory. Although non-linear evolution is extremely

complex, it is reasonable to assume that the constancy of the gravitational potential is approximately maintained even in the non-linear regime. For example, if one uses the spherical model (Peebles 1980) to study the non-linear evolution, then the gravitational potential changes only by a factor of 2 or so as the structures turn around, collapse and virialize. After the bound structures are formed, the virial theorem ensures that no significant evolution of the potential occurs. *In other words, the gravitational potential due to perturbations varies only by a factor of the order of unity when the density contrast changes from, say,* 10^{-4} *to* 10^{2}. We believe that this is an extremely important fact which can be profitably exploited to study non-linear evolution.

In order to implement this feature effectively, one can take a cue from another popular approximation scheme, usually called the Zeldovich approximation (Zeldovich 1970; Shandarin & Zeldovich 1989). In the Zeldovich approximation, one moves the particles using a fixed velocity field which is taken to be the initial velocity field. Mathematically, this scheme is implemented by assuming that

$$\boldsymbol{x}(t)=\boldsymbol{q}+a\boldsymbol{v}(\boldsymbol{q}), \tag{1}$$

where $\boldsymbol{q}$ is the Lagrangian coordinate of a particle, $\boldsymbol{x}$ is the co-moving Eulerian coordinate and $\boldsymbol{v}(\boldsymbol{q})=\mathrm{d}\boldsymbol{q}/\mathrm{d}a$ is the initial velocity field. This field $\boldsymbol{v}(\boldsymbol{q})$ is related to the gravitational potential ϕ by the relation

$$\boldsymbol{v}\equiv\nabla\Phi\equiv-\frac{2}{3a\dot{a}^{2}}\nabla\phi. \tag{2}$$

Because the Zeldovich approximation perturbs the trajectories rather than the density, it can be used to study a larger range of density contrast than the linear perturbation theory. Unfortunately, this approximation suffers from two significant shortcomings. The density contrast at any time, calculated from mass conservation, can be expressed as

$$\delta=\left[\prod_{i=1}^{3}(1-a\lambda_i)\right]^{-1}-1, \tag{3}$$

where λ_i are the eigenvalues of the matrix with elements $(-\partial v_i/\partial q_j)$, with $\lambda_1\geq\lambda_2\geq\lambda_3$. Hence, strictly speaking, the approximation breaks down when $a\lambda_1=1$, which occurs at fairly low density contrasts (say, around $\delta\simeq 2$) in realistic models.

A more serious shortcoming is the following: Zeldovich evolution gives a distorted view of the density distribution once pancakes form and particles move *through* the pancakes. Since the particles only 'remember' the *initial* velocities, they move past the pancakes unhindered, thereby leading to a fair amount of thickening of pancakes. Numerical simulations, on the other hand, clearly show that pancakes remain thin for long periods. We wish to emphasize that the question 'why do pancakes not thicken during the evolution of density perturbations?' is an important dynamical issue that needs to be understood from first principles. It is, of course, possible to introduce artificial models (such as the adhesion model, which contains damping mechanisms) that correctly reproduce the N-body results. The key question, in our opinion, is why models such as the adhesion model work as well as they do. In other words, there is something intrinsic in the gravitational dynamics of particles in an expanding universe that dampens the kinetic energy in the component perpendicular to the pancake more than the kinetic energy parallel to the pancake. This effect can be understood qualitatively as follows.

Consider a set of particles interacting via Newtonian gravity in an expanding universe. If we confine our attention to regions with dimensions much smaller than the Hubble radius, then the equation of motion for the ith particle is well approximated by

$$\ddot{\boldsymbol{r}}_{ij}=-\sum_{j\neq i}\frac{Gm}{|r_{ij}|^{3}}\boldsymbol{r}_{ij}\,;\qquad \boldsymbol{r}_{ij}=\boldsymbol{r}_i-\boldsymbol{r}_j. \tag{4}$$

Here $\boldsymbol{r}_i$ stands for the proper coordinate, related to the comoving coordinate $\boldsymbol{x}_i$ by $\boldsymbol{r}_i=a(t)\boldsymbol{x}_i$. In terms of $\boldsymbol{x}_i$, we have

$$\ddot{\boldsymbol{x}}_i+\frac{2\dot{a}}{a}\dot{\boldsymbol{x}}_i=-\nabla\phi, \tag{5}$$

where

$$\nabla^{2}\phi=\frac{4\pi G}{a^{3}}\left[\sum_j m\delta(\boldsymbol{x}-\boldsymbol{x}_j)-\rho_0 a_0^{3}\right]=4\pi G\rho_{\mathrm{b}}\delta \tag{6}$$

in the matter-dominated phase of the Friedmann model. In the above form the equations depend explicitly on t due to the presence of the terms $(\dot{a}/a)$ and a^3. This can be avoided by introducing new dimensionless time and space coordinates τ and $\boldsymbol{y}_i$ via

$$\tau\equiv\ln(t/T);\qquad \boldsymbol{x}_i\equiv L\boldsymbol{y}_i;\qquad L^{3}=Gmt_0^{2}/a_0^{3} \tag{7}$$

with an arbitrary constant, T. Transforming the equations, we easily find that

$$\frac{\mathrm{d}^{2}\boldsymbol{y}_i}{\mathrm{d}\tau^{2}}+\frac{1}{3}\frac{\mathrm{d}\boldsymbol{y}_i}{\mathrm{d}\tau}=-\nabla_{\mathrm{y}}U, \tag{8}$$

$$\nabla_{\mathrm{y}}^{2}U=4\pi\sum_j\delta(\boldsymbol{y}-\boldsymbol{y}_j)-\frac{2}{3}. \tag{9}$$

Equation (8) can be used to understand the motion of the particles near a pancake. Locally, the gravitational acceleration, $\boldsymbol{g}=-\nabla U$, is towards the pancake and has no appreciable component parallel to the pancake. Hence the velocity parallel to the pancake ($v_{\parallel}$) decays as a result of cosmic expansion alone [described by the $(1/3)\dot{\boldsymbol{y}}$ term], while the velocity normal to the pancake ($v_{\perp}$) is affected by the potential as well. It turns out that this effect restricts the motion in the direction perpendicular to the pancake (see Fig. 5 and our discussion later). Quite clearly, the local gravitational force produced by the pancake plays an important role in this process. Since the Zeldovich approximation misses out the effects of acceleration and evolves particles using the initial velocity field, it fails to reproduce the thin nature of the pancakes.

The above discussion suggests a possible new way of approximating non-linear evolution. The success of the Zeldovich approximation clearly demonstrates that one should work in a Lagrangian description and consider the perturbation of trajectories. However, it is also necessary that the effect of acceleration is incorporated into this scheme. In a rigorous N-body simulation, this is done by using the *exact*

gravitational force acting on the particle at every instant of time. If, however, our hypothesis of approximate constancy of the gravitational potential is correct, then one should be able to make considerable progress by evolving the trajectories using a pre-specified gravitational potential that remains frozen in time. This is the idea that we pursue here.

The Euler equation governing the motion of fluid particles can be written in the comoving coordinates as

$$\frac{d\boldsymbol{v}}{da} = -\frac{3}{2a}[\mu\nabla\phi + \boldsymbol{v}], \tag{10}$$

where the velocity is defined as $\boldsymbol{v} = d\boldsymbol{x}/da$ and μ is a constant that equals $(2/3a\dot{a}^2)$. The left-hand side of equation (10) is, of course, the convective derivative evaluated along the path of the particle. In the proposed scheme we use Euler's equation with the potential as specified at the initial time. The initial velocity of a particle is assumed to be $-\mu\nabla\phi$, just as in the Zeldovich approximation. At subsequent instants of time, the acceleration is computed by using the *instantaneous* velocity of the particle and the *initially specified* potential at its *current* position. In reality, the potential will also change with time as the density distribution evolves. It is this fact that we ignore by invoking the hypothesis of constancy of the potential.

We find that this approximation works well and that the pancakes do not thicken. The particles tend to move along the pancakes towards regions of lower potential to end up in a few clumps. The acceleration we use in this approximation is largest in regions where the instantaneous velocity vector points along the gradient of the potential, as happens for particles after they cross the pancake.

This may be thought of as a 'frozen potential' formulation for the evolution of density perturbations. Recently, Matarrese et al. (1992) proposed a frozen flow approximation (FFA), which essentially freezes the velocity field rather than the potential. In this approach the particles move along streamlines computed from the initial potential, using the same relation as in the Zeldovich approximation (equation 2). Here, however, the inertia of particles is ignored, whereas in the Zeldovich approximation inertia is assumed to dominate over change in the force field. We take into consideration both factors but assume a constant potential. As we shall see, our approximation provides more accurate velocity information and a more accurate dynamical picture than the FFA.

3 SIMULATION RESULTS AND DISCUSSION

The idea was explored numerically in the following manner. We start with an initial potential ϕ (in 3D with a $128\times128\times128$ grid) which is a realization of a Gaussian random field with the power spectrum $P_\phi \propto P_\delta(k)/k^4$, where $P_\delta(k)$ is the power spectrum for density. We investigate standard cold dark matter (CDM) and hot dark matter (HDM) models, as well as two power-law spectra with indices $n=1, -2$. These examples are chosen to give the widest possible coverage that is realistic. The particles are now moved by the ansatz described above. We normalize our expansion factor such that $a=1$ at the present epoch. We shall now discuss several results and compare them with different approximations and exact N-body results.

To begin with, Figs 1–4 give slices of the Universe in various approximation schemes at different epochs from the spectra mentioned above. In Fig. 1 we show the evolution for the standard CDM model normalized to *COBE*. The top three frames are based on our approximation, the middle three are based on frozen flow and the bottom ones are obtained using the Zeldovich approximation. The time evolution proceeds from left to right across the frames, and these correspond to $a=0.25$, 0.5 and 1.0. The slices in the frames have dimensions $96\ h^{-1}$ Mpc $\times 96\ h^{-1}$ Mpc $\times 15\ h^{-1}$ Mpc. Fig. 2 shows the corresponding results for the HDM model. (Since the HDM model normalized to *COBE* produces non-linear structures only around $a\simeq1$, we have evolved the simulations up to $a=2$ in this case.) Figs 3 and 4 give the results for the power-law spectra $[P_\delta(k)\propto k^n]$ with indices $n=1, -2$. These are normalized by the condition $\sigma_8=1.0$.

It is quite obvious that the Zeldovich approximation is the worst of the three for $a\gtrsim1$. The pancakes thicken enormously and, of course, this is to be expected, since we are continuing the trajectories beyond the shell crossing. The top and middle frames show that there is some superficial similarity between the spatial distributions calculated by frozen flow and frozen potential. There is, however, a significant difference in the details. The velocities of particles in the non-linear regimes (and the nature of their motion near pancakes) are quite different in the two cases. In frozen flow, no shell crossing occurs and the particles approach the pancakes more and more slowly. In the FPA, there is shell crossing and significant motion near the pancakes. In order to show this difference clearly, we have plotted the 2D trajectories of a few particles near the pancakes in Fig. 5. In the frozen flow, trajectories approach one another asymptotically, thereby defining the 'pancakes' (thin lines in Fig. 5). In the FPA (thick lines), however, the particles cross the pancake and oscillate around the plane because of the local acceleration. It is this feature that limits the thickness of the pancake. The pancake in Fig. 5 forms around $a=1$, but the trajectories are evolved for a much longer time to show that particles remain confined in the pancake. One can also see that the results of our approximation are similar to those of N-body simulations, and that in evolving from $a=0.5$ to $a=1.0$ the particles form more clumpy regions in comparison with FFA. We shall now contrast the three approximations and also compare the FPA with N-body results.

The nature of these approximations – Zeldovich, frozen flow and frozen potential – can be compared qualitatively in the following simple manner. Let $\boldsymbol{v}(\boldsymbol{q})$ be the initial velocity field, which we start with as a realization of some given power spectrum. Suppose that, by random occurrence, all the velocity vectors in some given, finite subregion of space point roughly towards a plane (on both sides). Quite clearly, particles in that region will move towards this plane and, in the Zeldovich approximation, we will obtain a pancake coinciding with the plane. When we evolve the system further (using the Zeldovich approximation) the particles will continue to move with their *original* velocities. This will result in the particles crossing the plane and moving away from it, and a consequent thickening of the pancake.

In the FFA, the *local* velocity field is used to move the particles (rather than the *initial* velocity field at the original Lagrangian coordinate). For this velocity field, which

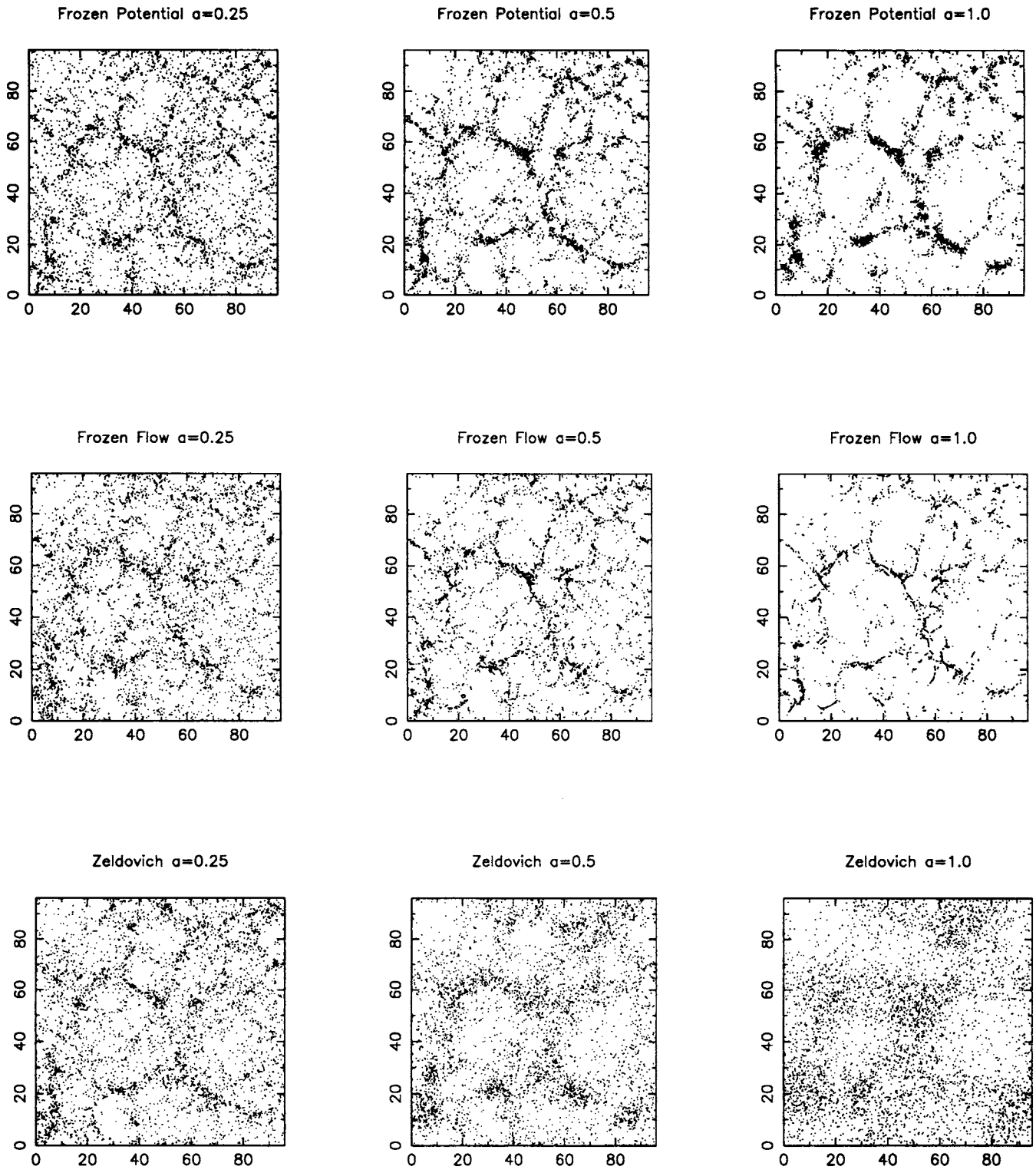

Figure 1. Evolution of density perturbations in CDM for various approximations. These frames, from left to right, correspond to $a = 0.25$, 0.5 and 1.0 (present epoch) respectively. The top row of frames shows evolution according to the frozen potential approximation, the middle row shows that for the frozen flow approximation, and the bottom row that for the Zeldovich approximation.

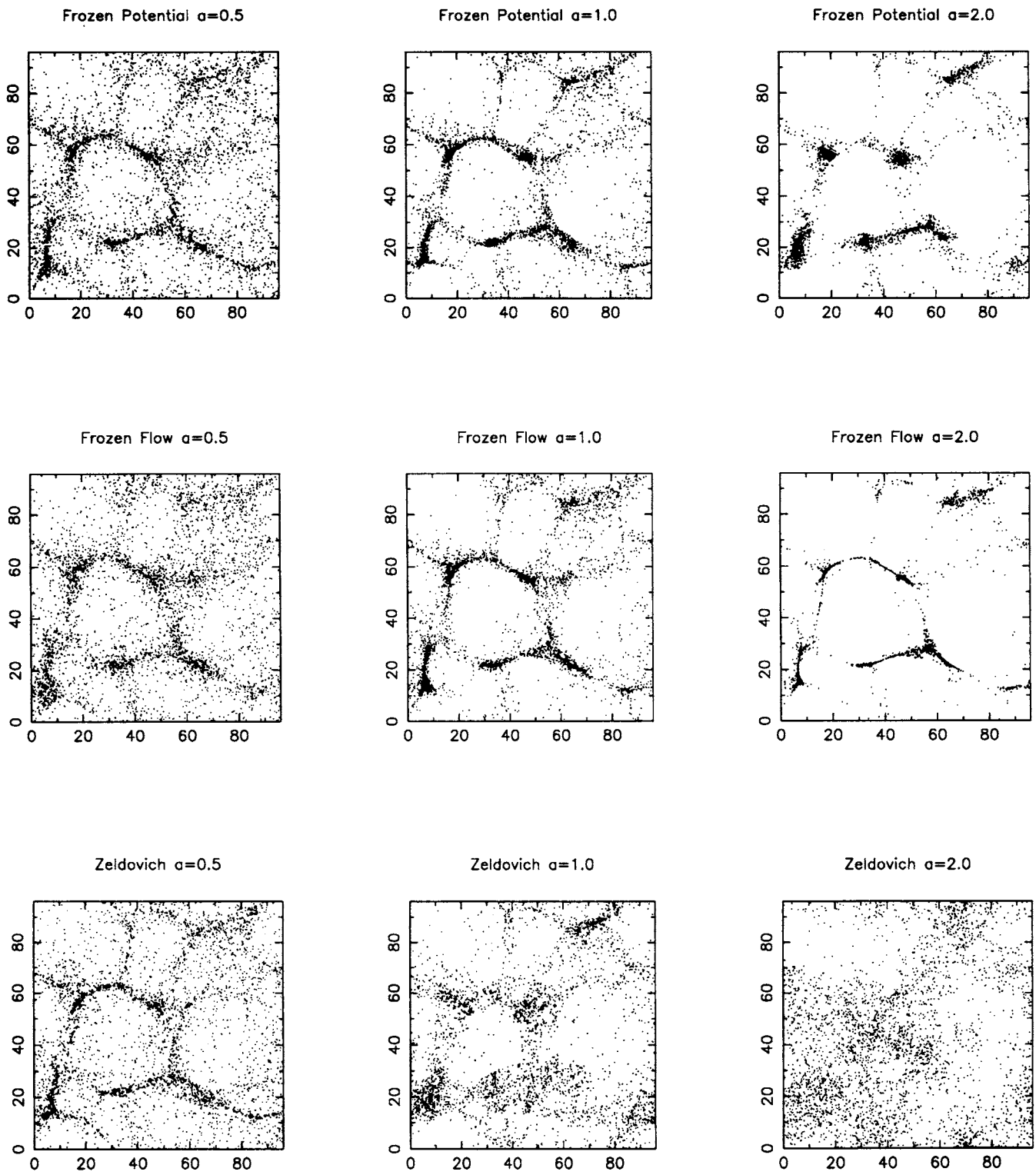

Figure 2. Same as Fig. 1, but for HDM ($a = 0.5$, 1.0 and 2.0).

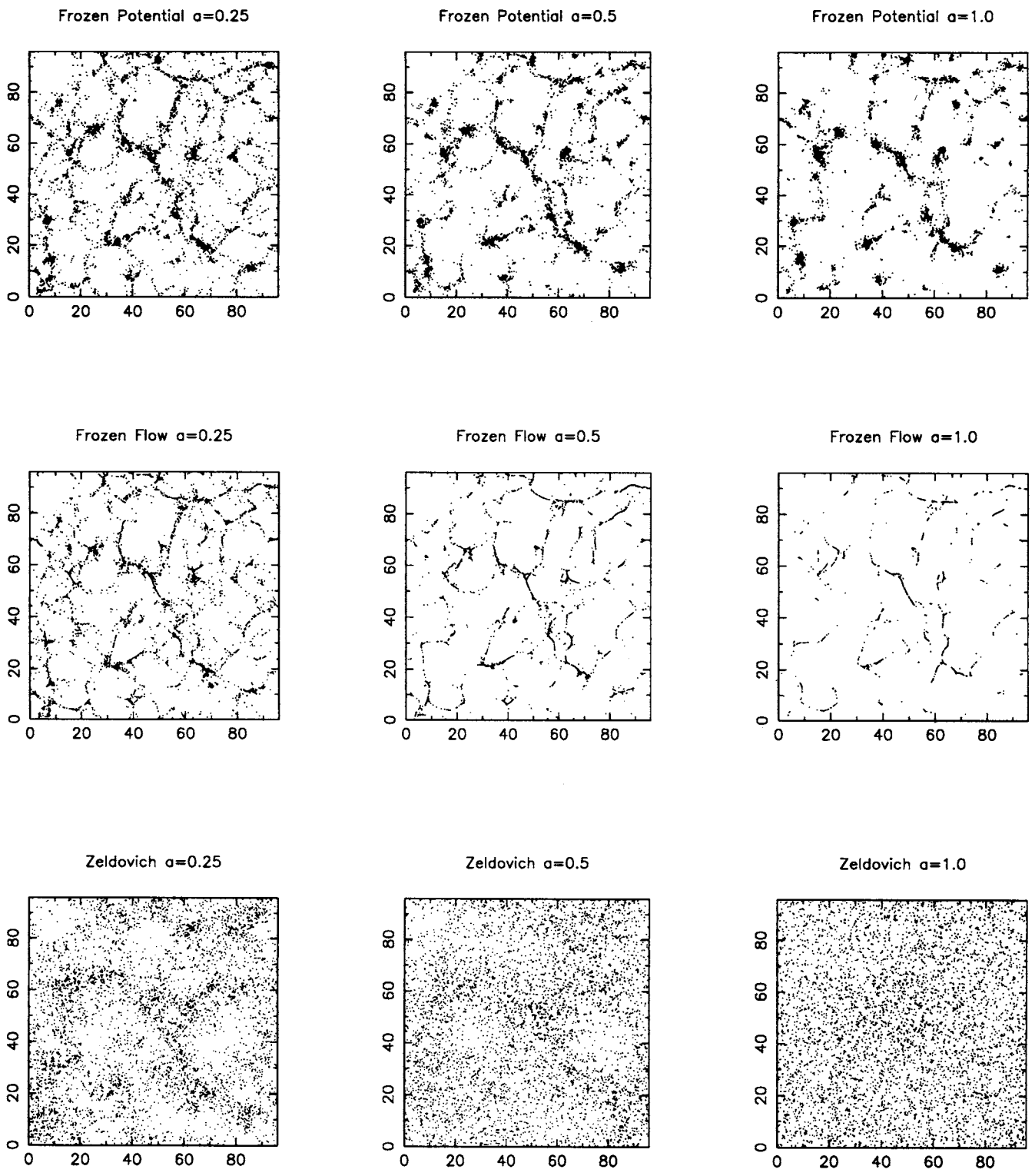

Figure 3. Same as Fig. 1, but for the Zeldovich–Harrison spectrum ($n = 1$).

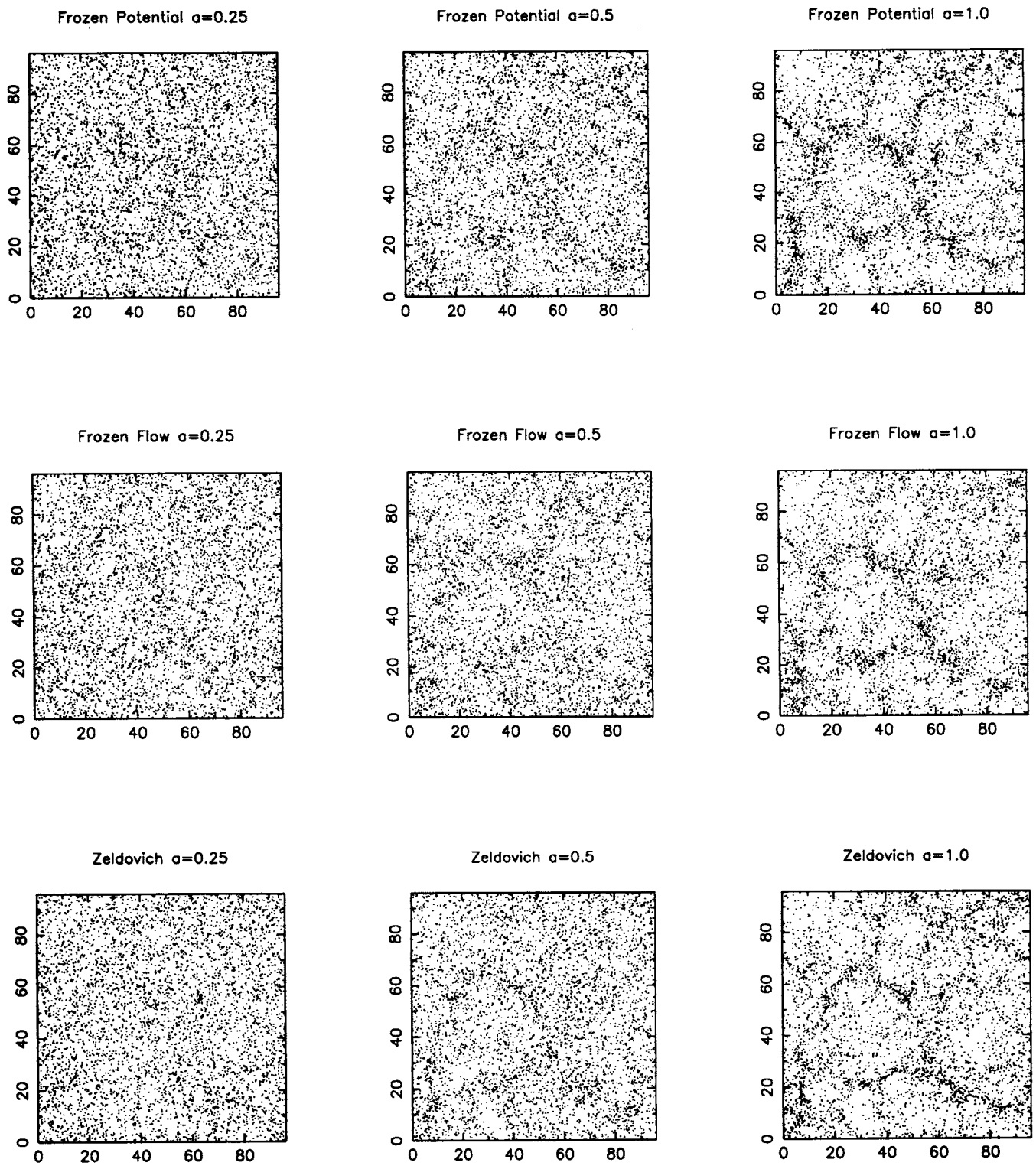

Figure 4. Same as Fig. 1, but for $n = -2$.

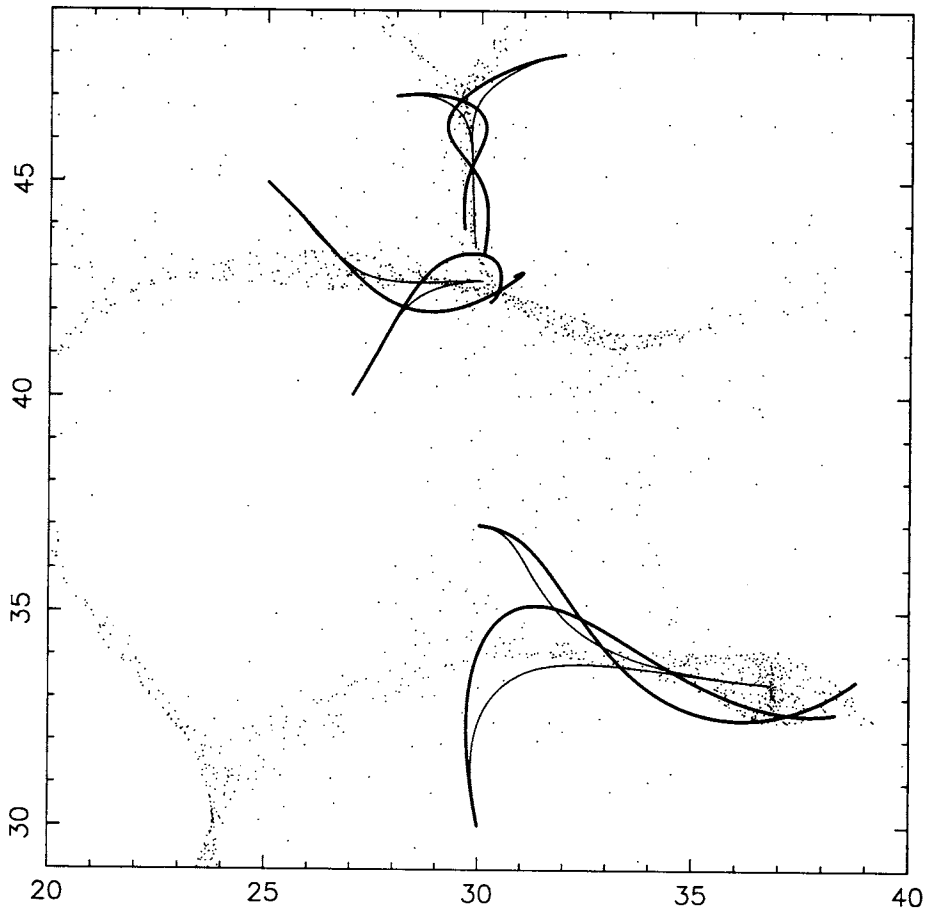

Figure 5. Trajectories of a few particles near pancakes. The pancakes have formed at $a \simeq 1$ but the trajectories are evolved for a much longer time to show that particles remain confined in the pancakes. Thin lines correspond to trajectories in the frozen flow approximation and thick lines to trajectories in the frozen potential approximation.

is generally pointing towards a plane, continuity demands that the velocities become smaller and smaller near the plane. This means that the velocities of particles normal to the plane will become smaller and smaller as they approach the would-be pancake. Quite obviously, no thickening of the pancake will take place, since no pancake has really formed.

In the frozen potential formulation, the evolution is quite different. Along with the initial velocity field, we also have an initial acceleration field, $\boldsymbol{g}$, defined in that region. Since the density contrast was small at the initial epoch, allowing the use of linear theory, we know that $\boldsymbol{g} = -\mu\nabla\phi$ and $\boldsymbol{v}$ point in the same direction. In other words, the acceleration vector field also points towards the plane. If we evolve the particles using the acceleration field, then the particles that cross over the pancakes get pushed back towards them. This force prevents the particles from moving too far away from the pancakes; consequently the pancakes remain thin.

We stress that in FFA no actual shell crossing can occur. Thus, even though the FFA prevents thickening of pancakes, it does so in a somewhat crude manner. In the case of the FPA, shell crossing does occur but the particles are dynamically influenced by the gravitational potential, which reverses their direction of motion when they cross the pancake. [The complete velocity information and shell crossing are important dynamical features of our approximation, but in some cases this extra information can become a liability, as in reconstruction of initial conditions.]

It is also possible to understand these features by the following simple example. Suppose that, around some region of the space, the initial gravitational potential is that of a constant-density ellipsoid:

$$\phi(\boldsymbol{x}) = \frac{1}{2}(\omega_x^2 x^2 + \omega_y^2 y^2 + \omega_z^2 z^2). \tag{11}$$

By taking different relative values for the three frequencies, we can simulate regions which vary from a sphere to a flat pancake. It is easy to work out the trajectories of particles in this potential in all three approximations. In the Zeldovich approximation, the peculiar velocity depends only on the starting point of the particle and the epoch. Thus we have for the velocity

$$v_i = -\mu\omega_i^2 x_i^{IN}, \tag{12}$$

where $i = 1, 2, 3$ and the superscript IN denotes the initial values. For this trajectory, this gives us

$$x_i = x_i^{IN} + a v_i. \tag{13}$$

Thus the trajectory is just a straight line, with peculiar velocity depending only on the initial point.

In the FFA, the velocity is a function of the instantaneous coordinates of the particle only. For the ith direction, we can write

$$v_i = -\mu\omega_i^2 x_i. \tag{14}$$

Solving the equation, $u_i = \mathrm{d}x_i/\mathrm{d}a = -\mu\omega_i^2 x_i$, we obtain the trajectory of the particle to be

$$x_i = x_i^{IN} \exp(-\mu\omega_i^2 a). \tag{15}$$

The particle approaches the mass concentration asymptotically with a decaying velocity.

On solving equation (10) with the potential frozen to equation (11), the frozen potential ansatz gives the following result for the velocity and the trajectory along the ith axis:

$$v_i = -\frac{x_i}{a} + \frac{\sqrt{6\omega_i^2\mu}}{2a}\left[B\cos(\sqrt{6\omega_i^2\mu a}) - A\sin(\sqrt{6\omega_i^2\mu a})\right] \tag{16}$$

and

$$x_i = \frac{1}{\sqrt{a}}\left[A\cos(\sqrt{6\omega_i^2\mu a}) + B\sin(\sqrt{6\omega_i^2\mu a})\right]. \tag{17}$$

Now consider the special case of a plane symmetric (axisymmetric) potential. Here the symmetry of the mass distribution requires ω_i to be vanishingly small in the direction parallel to the plane (parallel to the axis of symmetry). Then the above equation implies that, in the FPA, the velocity of the particles in this direction decays as $a^{-3/2}$. This can be seen easily, as only the first term in equation (16) contributes, giving the above-mentioned dependence. The frozen flow ansatz predicts zero velocity in such a case, as does the Zeldovich approximation. In the direction normal to the plane (transverse to the axisymmetric) distribution, the FFA gives a velocity proportional to the distance from the plane (axis) of symmetry, directed towards it. In the Zeldovich approximation the trajectories point towards the potential minima initially, but after shell crossing the particles retain their initial velocities and this leads to thickening of the pancakes/filaments. The FPA, on the other hand, gives damped oscillating trajectories about the mass distribution, and therefore the trajectories of particles remain confined.

Having compared the three approximations, let us now turn to the question of the limits of validity of the FPA. There is one basic limitation in any approximation that freezes physical variables in the Euler space. In the FPA, the large-scale structures like voids and filaments can be traced back to the location of the turning points in the gradient of the initial potential. This implies that the motion of these large-scale structures is not adequately taken into account in our approximation. In standard CDM, for example, the streaming velocity at about 50 h^{-1} Mpc is about 200 km s^{-1}. Therefore these structures could have moved a distance of about 2 h^{-1} Mpc within the Hubble time. Thus one would expect the FPA to show deviations from N-body results at around 2 h^{-1} Mpc. Although this argument is correct, the numerical estimate is accurate only within an order of magnitude because of several uncertainties in the definitions, etc. However, Brainerd et al. (1993) compared the frozen potential with the exact N-body potential, and did indeed find that the deviations occur on approximately this scale.

This, of course, is only part of the story. In the FPA the depths of potential wells are decided beforehand and particles move towards the minima of these potential wells. In reality, however, the clustering of the particles will cause the depths of the potential wells to increase in the non-linear regime, which is not taken into account by the FPA. This also means that the FPA will underestimate the relative pair velocities of particles compared to the actual N-body result.

It is possible to provide a very illuminating comparison between the actual N-body results and the FPA using certain universal relations that are independent of the power spectra as well as the epoch under consideration. These universal relations involve the scaled average pair velocity, $h(a, x) \equiv [-v_{\mathrm{pair}}(a, x)/\dot{a}x]$, and the averaged two-point correlation function $\bar{\xi} = 3x^{-3}J_3 = \langle(\delta M/M)^2\rangle$. Theoretical reasoning (see Nityananda & Padmanabhan 1993; Padmanabhan 1992) as well as results of numerical simulations (Hamilton et al. 1991) suggest the following. (i) The function $h(a, x)$ depends on a and z only through $\bar{\xi}$, i.e. $h(a, x) = h[\bar{\xi}(a, x)]$, where the form of this function is universal; that is, it is the same for a wide variety of power spectra at different epochs. (ii) $h \simeq (2/3)\,\bar{\xi}$ for $\bar{\xi} \ll 1$, *rises to a value greater than unity*, and falls to unity for $\bar{\xi} \gg 1$. It is possible to show that this function $h(\bar{\xi})$ contains the necessary information to extract the exact non-linear density contrast from the density contrast of the linear theory. The relation between the true $\bar{\xi}$ and the $\bar{\xi}_L$ calculated from the linear theory is given by (see for example Hamilton et al. 1991)

$$\bar{\xi}_L(a, l) = \exp\left(\frac{2}{3}\int_0^{\bar{\xi}} \frac{\mathrm{d}y}{h(y)(1+y)}\right), \tag{18}$$

with

$$l^3 = x^3(1 + \bar{\xi}(x)). \tag{19}$$

The N-body simulations can be fitted very well by the following choice for $h(\bar{\xi})$ (see Hamilton et al. 1991):

$$h(\bar{\xi}) = -\frac{2}{(1+\bar{\xi})}\frac{f_1(\bar{\xi})}{f_2(\bar{\xi})}, \tag{20}$$

where

$$f_1(y) = y + 0.9418\,y^3 - 0.0742\,y^4 + 0.03023\,y^5 - 0.001067\,y^6 + 0.000238\,y^7 + 0.000001794\,y^8$$

and

$$f_2(y) = 3 + 1.005\,y^2 + 0.00069\,y^3 + 0.0282924\,y^4 - 0.0019219\,y^5 + 0.0002208\,y^6 + 0.000003588\,y^7.$$

By comparing this N-body result with the FPA and FFA we can clearly understand what happens in the non-linear regime. This comparison has the advantage that it is independent of the specific power spectrum that is being studied.

The results of such a comparison are shown in Fig. 6(a), which plots $h(\bar{\xi})$ for the FPA, FFA and N-body simulations. It is clear that the FFA has the wrong shape at non-linear densities when compared to the N-body result. The FPA, on the other hand, has the correct overall shape but deviates from the N-body result in two significant ways. First, it does not rise as much as the N-body curve does. This is because the potential depth does not increase in the FPA as much as in N-body simulations. Secondly, the FPA curve does not

saturate precisely at unity. Because of these two effects, it is clear that the FPA will underestimate the non-linear density compared to *N*-body simulations. (The second feature, however, cannot be completely settled because all simulations have a resolution limit at small scales. The *N*-body curve, for example, is affected by the smoothing scale used in the potential at high densities.) The following point can, however, be made: when virialized systems form, the ratio between the final values of kinetic and potential energies will be different for self-gravitating systems and systems in an external potential. By analogy, we expect the final value of h to be different (though of the same order) in the FPA from in *N*-body simulations. Other effects, however, are likely to invalidate the approximation before this effect becomes crucial.

Finally, it is clear from Fig. 6(a) that the FPA gives better velocity information than the FFA even in the non-linear regime; this, of course, is to be expected because of the nature of the approximation. [Incidentally, we verified that both the approximations lead to the same h for different power spectra and epochs, though the form of the curve is different from that of the *N*-body result; this fact has important implications for the statistical mechanics of particles in external potentials and we will address this question in a future publication (Bagla & Padmanabhan, in preparation).] Fig. 6(b) is a plot of the averaged correlation function with its linear counterpart at scales related by equation (19). The FPA has broadly the correct shape but underestimates the non-linear density contrast. The FFA, on the other hand, does not lead to the correct shape or the magnitude of pair velocity in the non-linear regime.

Fig. 7 shows these effects in the context of density contrast in CDM (normalized to *COBE*). The curves show the evolution of density contrast in the FPA and compare the density contrast at $z=0$ with the exact *N*-body result. Clearly, the FPA underestimates the density contrast at small scales but does reasonably well in the quasi-linear regime. In Fig. 8 we compare the results of the FFA and the FPA with the exact *N*-body result. The FFA overestimates the non-linearities significantly, while the FPA underestimates them; this is, of course, evident from the velocity information in Fig. 6(a).

The approximation suggested here could also replace the adhesion model in some contexts. It may be recalled that the adhesion model (with an artificial viscosity term) was originally introduced to keep the pancakes thin and to provide information regarding the locations of the pancakes. The approach described here keeps the pancakes thin because of natural, dynamical reasons eliminating the need for the introduction of a viscosity term. The approach can also provide the location of pancakes. What is more, the code for the present approximation is both conceptually and numerically simple to implement as compared to the adhesion code. The formation and properties of the voids, for example, can be studied quite easily by this approach.

The approximation outlined in this paper is ideally suited to study another important problem: the dynamics of baryons in dark matter potential wells. At present, attacking this problem using *N*-body simulations is extremely hard and

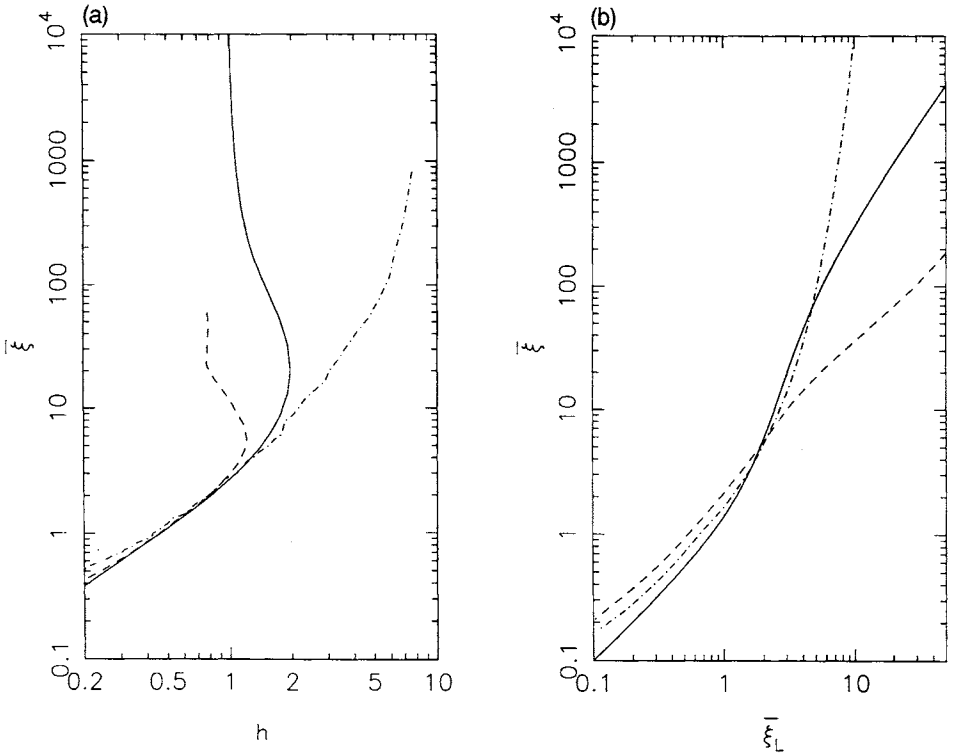

Figure 6. Comparison with *N*-body simulations. The solid curve is a fit to the *N*-body simulations given by Hamilton et al. (1991). The dashed curve corresponds to the FPA and the dot–dashed curve is for the FFA. These curves have the same form at all epochs and for a range of power spectra. (a) The ratio of the relative pair velocity to the Hubble velocity, averaged over pairs of particles, is plotted as a function of $\bar{\xi}$ on the relevant scale. (b) The universal relation between the $\bar{\xi}_L$ obtained from linear theory and the non-linear $\bar{\xi}$ obtained from simulations is shown in this curve. Note that $\bar{\xi}$ and $\bar{\xi}_L$ are calculated on different scales given by equation (19).

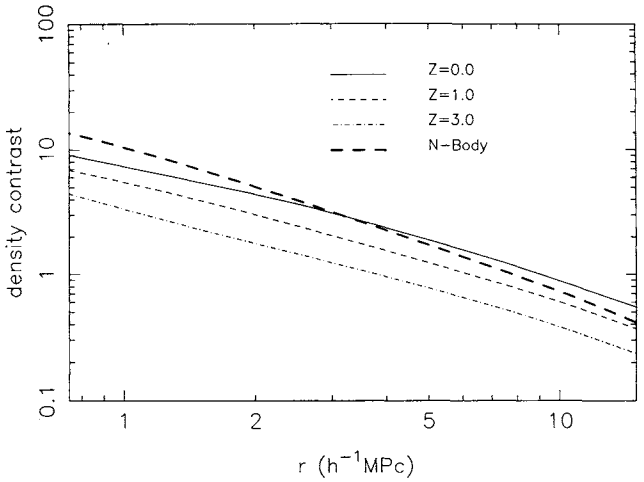

Figure 7. Evolution of density contrast in the FPA. Also drawn here is the density contrast obtained from *N*-body simulations at $z=0$. Here the density contrast is defined as $\sigma \equiv \sqrt{\bar{\xi}}$.

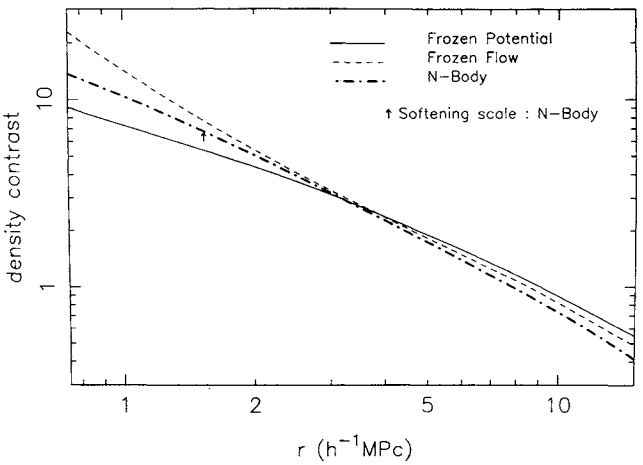

Figure 8. Density contrast in various approximations and in *N*-body simulations.

time-consuming. Approximation schemes such as the adhesion model will not be useful in this context; the FFA, on the other hand, will provide a distorted picture of the motion near pancakes. The FPA, with its better velocity information, may give us valuable insights into the physical processes at work while economizing greatly on the computation involved.

ACKNOWLEDGMENTS

The authors thank K. Subramanian for useful discussions and the referee for several constructive comments. One of us (JSB) would like to thank Varun Sahni for introducing him to quasi-linear approximation. JSB is being supported by the Junior Research Fellowship of the Council of Scientific and Industrial Research, India.

REFERENCES

Brainerd T. G., Scherrer R. J., Villumsen J. V., 1993, ApJ, in press
Hamilton A. J. S., Kumar P., Lu E., Matthews A., 1991, ApJ, 374, L1
Matarrese S., Lucchin F., Moscordini L., Saez D., 1992, MNRAS, 259, 437
Nityananda R., Padmanabhan T., 1993, MNRAS, submitted
Padmanabhan T., 1992, Current Science, 63, 379
Peebles P. J. E., 1980, Large Scale Structure of the Universe. Princeton Univ. Press, Princeton, NJ
Shandarin S. F., Zeldovich Ya. B., 1989, Rev. Mod. Phys., 61, 185
Zeldovich Ya. B., 1970, A&A, 5, 84